Particle acceleration from an inner accretion disc into compact corona and further out

Case of an organised magnetic field near a SMBH

Vladimír Karas[1]

in collaboration with

O. Kopáček,[1] J. Kovář,[2] Y. Kojima[3]

[1]Astronomical Institute, Czech Academy of Sciences, Prague

[2]Institute of Physics, Silesian University, Opava

[3]Department of Physics, Hiroshima University

9th FERO Meeting – Finding Extreme Relativistic Objects, Heraklion (Crete), 23–25 May 2018

Outline

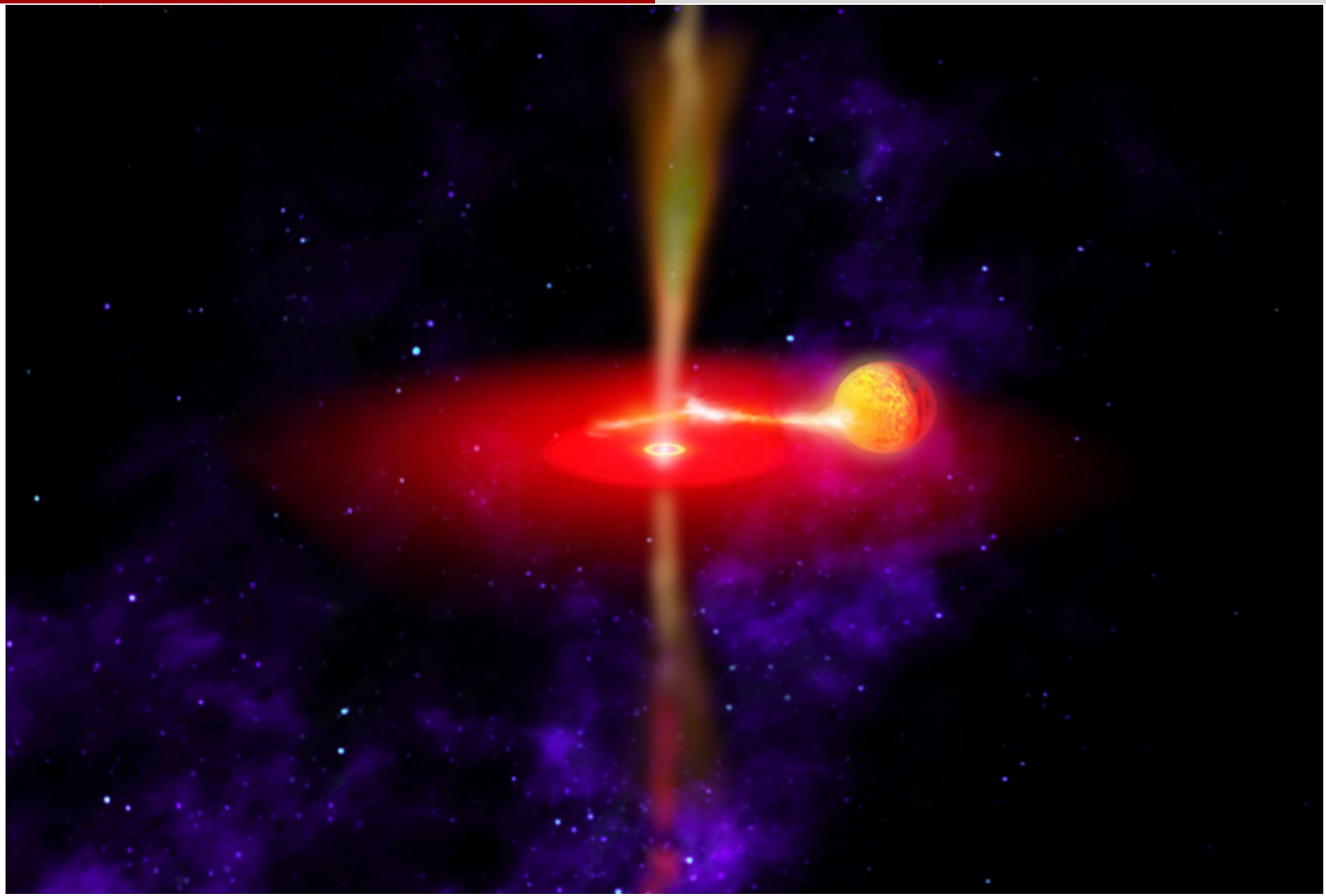

(Picture credit: Dana Berry)

Formal description of the model

- Kerr metric $x^\mu = (t,\ r,\ \theta,\ \varphi)$:

$$ds^2 = -\frac{\Delta}{\Sigma}\left[dt - a\sin\theta\, d\varphi\right]^2 + \frac{\sin^2\theta}{\Sigma}\left[(r^2+a^2)d\varphi - a\, dt\right]^2 + \frac{\Sigma}{\Delta}\, dr^2 + \Sigma d\theta^2,$$

where

$$\Delta \equiv r^2 - 2Mr + a^2, \quad \Sigma \equiv r^2 + a^2\cos^2\theta.$$

  - aligned with the symmetry axis: Wald (1974), King et al (1975)
  - a general (mis-aligned) orientation: Bičák et al. (1985)

$$\begin{aligned}
A_t &= \frac{B_\perp aMr}{\Sigma}\left(1+\cos^2\theta\right) - B_\perp a + \frac{B_\parallel aM\sin\theta\cos\theta}{\Sigma}\left(r\cos\psi - a\sin\psi\right) - \frac{Qr}{\Sigma} \\
A_r &= -B_\parallel (r-M)\cos\theta\sin\theta\sin\psi \\
A_\theta &= -B_\parallel a(r\sin^2\theta + M\cos^2\theta)\cos\psi - B_\parallel (r^2\cos^2\theta - Mr\cos 2\theta + a^2\cos 2\theta)\sin\psi \\
A_\varphi &= B_\perp \sin^2\theta\left[\frac{1}{2}(r^2+a^2) - \frac{a^2Mr}{\Sigma}(1+\cos^2\theta)\right] - B_\parallel \sin\theta\cos\theta\left[\Delta\cos\psi + \frac{(r^2+a^2)M}{\Sigma}(r\cos\psi - a\sin\psi)\right] \\
&\quad + \frac{Qra\sin^2\theta}{\Sigma}.
\end{aligned}$$

Poloidal sections across regions of stable motion

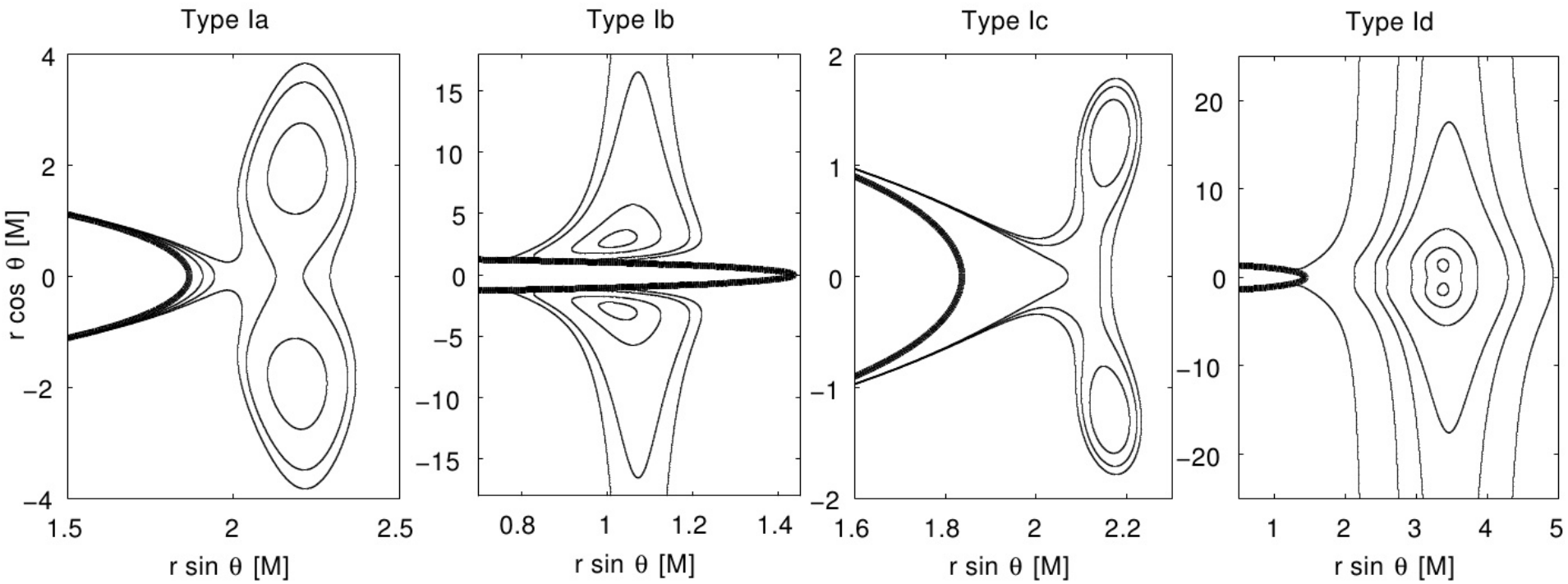

A magnetized black hole embedded in an organized poloidal component: classification of possible topology (Kovář et al. 2010).

Chaotic escape from the accretion disk

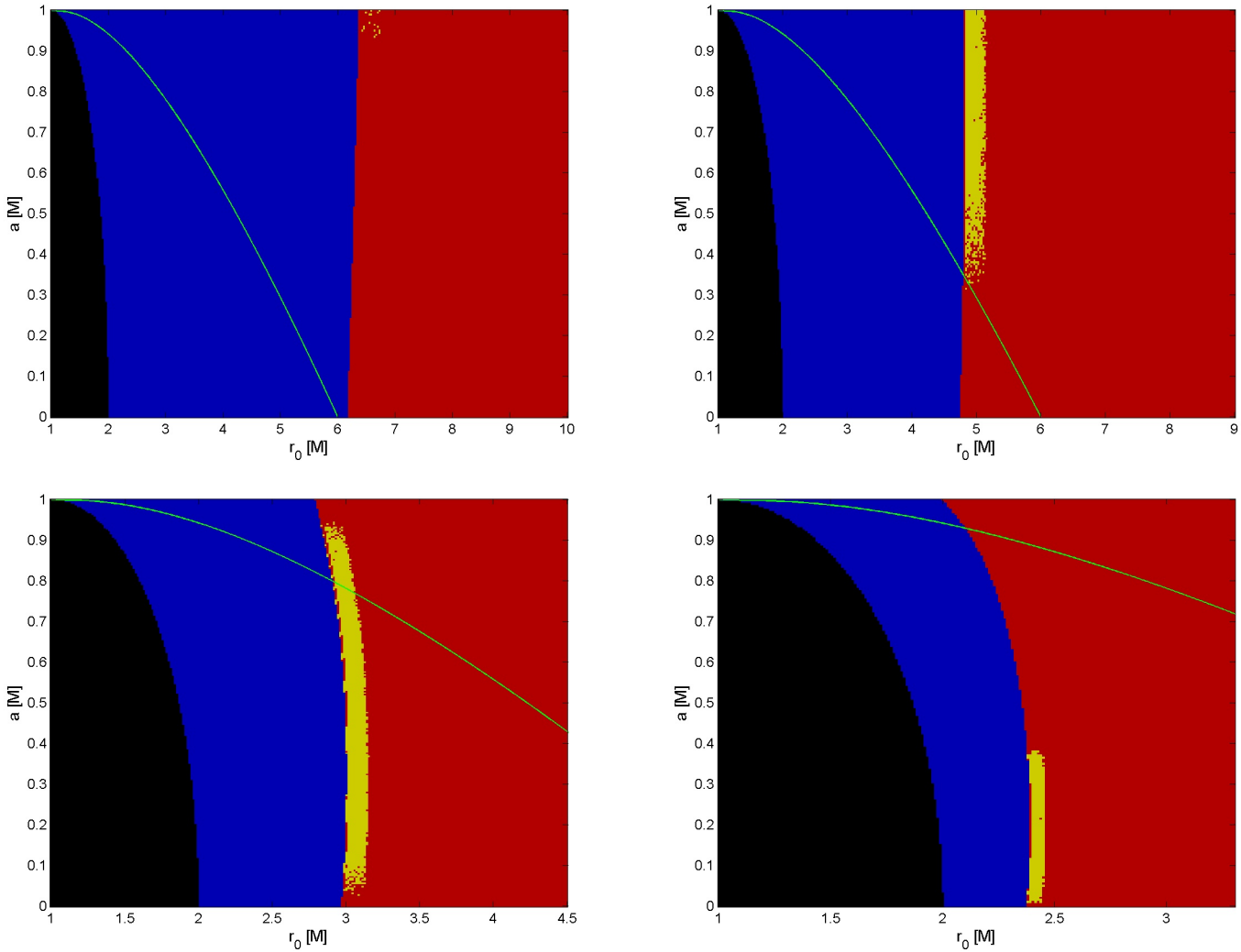

Spin a vs. radius r – zones of chaos (different values of qB).

Chaotic escape from the accretion disk – detail

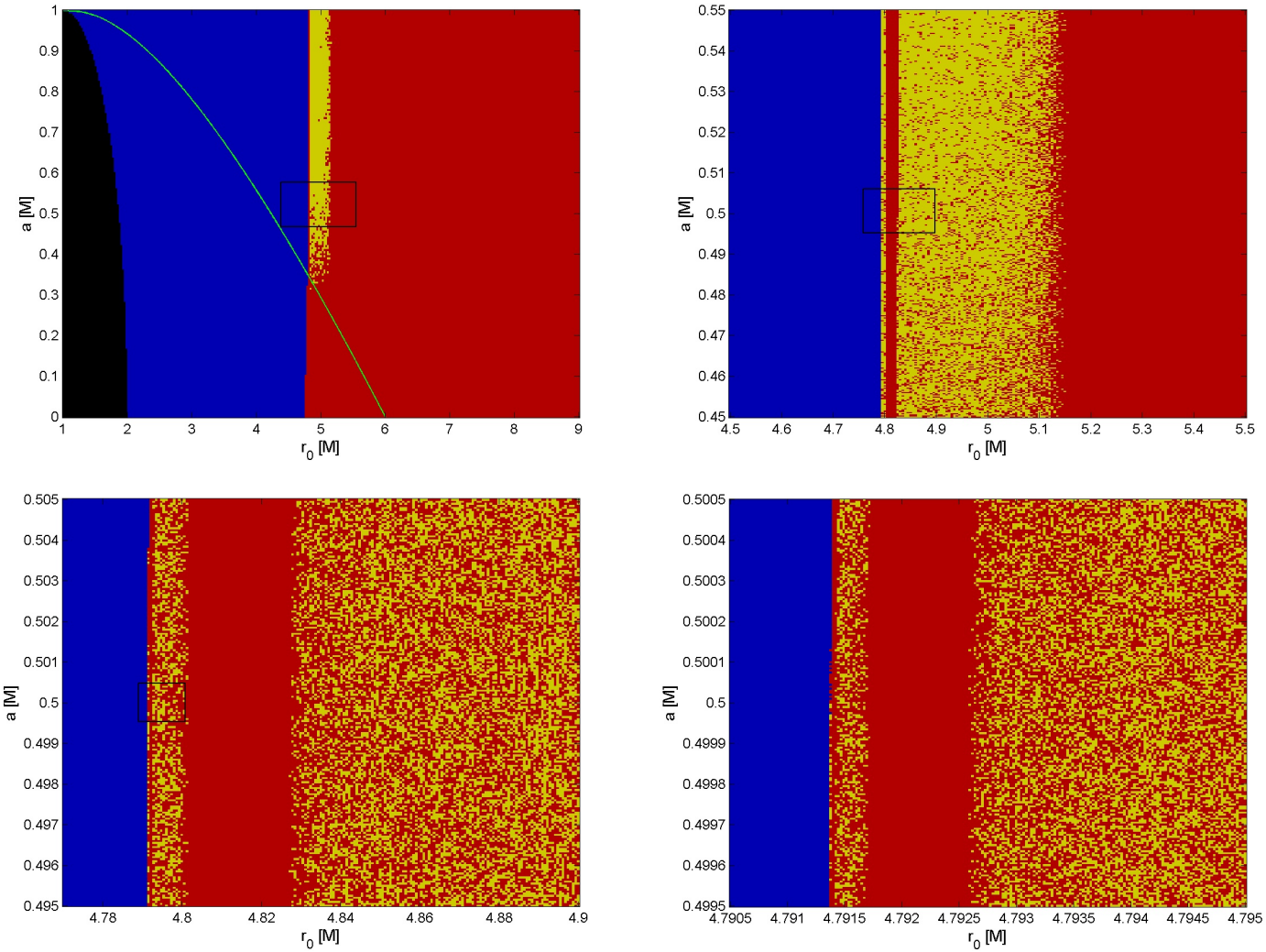

Escape zone is densely populated by both the chaotic escaping (yellow) orbits *and* the regular (red) orbits oscillating near the equatorial plane.

Chaotic escape from the accretion disk – acceleration

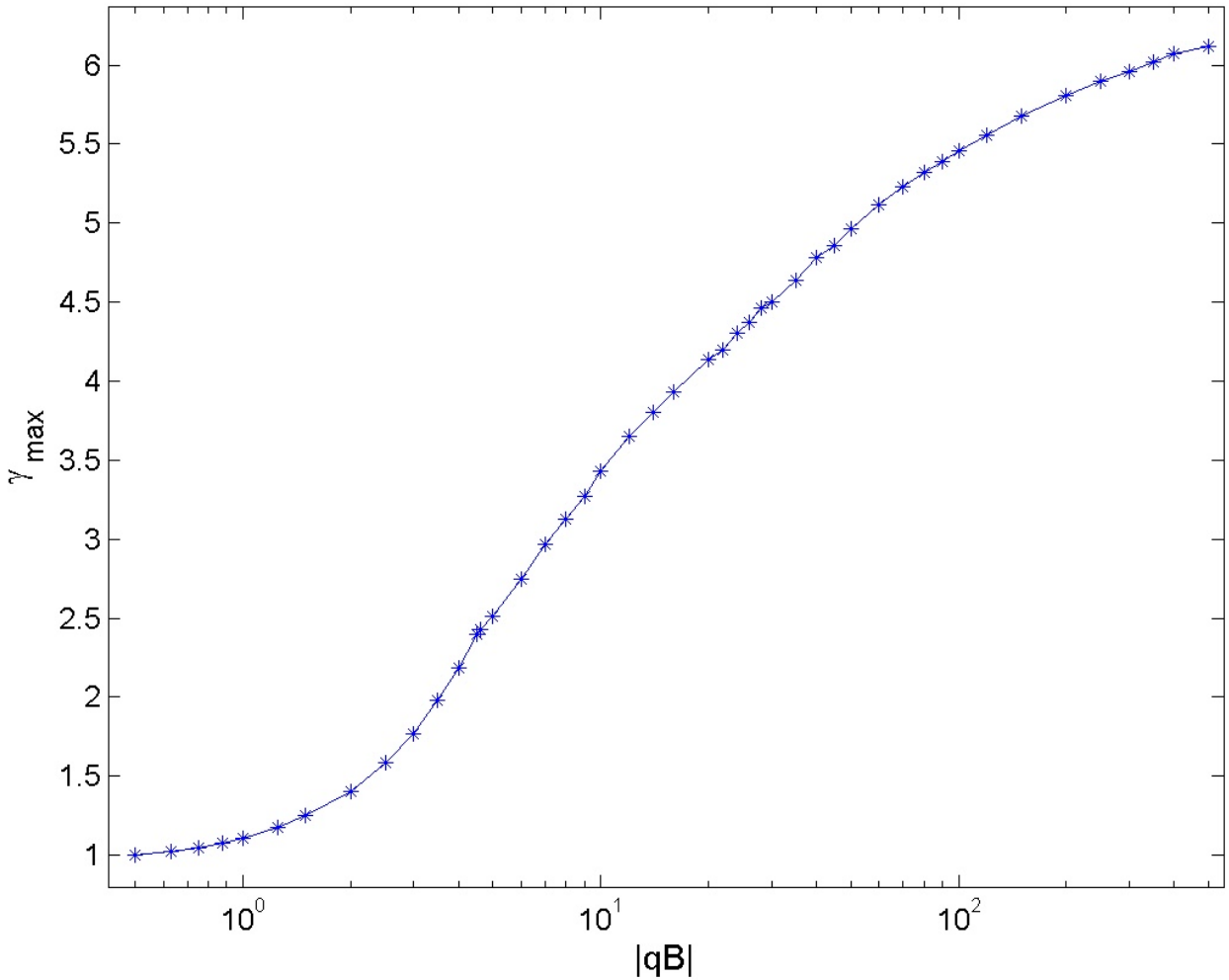

Acceleration of the escaping particles changes with the BH spin.
Terminal velocity grows with the magnetization $|qB|$.

Recurrences as an approach complementary to Poincaré sections and Lyapunov coefficients

Formal definition

Binary valued Recurrence Matrix $\mathbf{R}_{ij}$ from the phase space trajectory $\vec{x}(\tau)$:

$$\mathbf{R}_{ij}(\varepsilon) = \Theta(\varepsilon - ||\vec{x}(i) - \vec{x}(j)||), \quad i, j = 1, ..., N$$

- Θ – Heaviside step function
- ε – threshold parameter – controls density of $\mathbf{R}_{ij}$
- N – sampling frequency of examined time period
- $||.||$ norm applied to the phase space

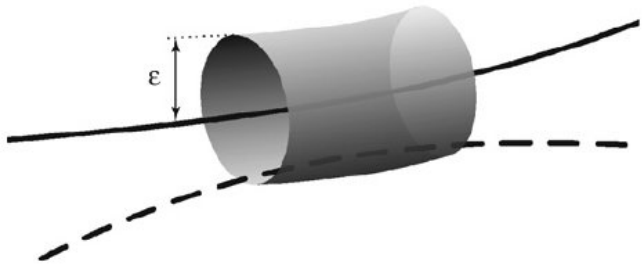

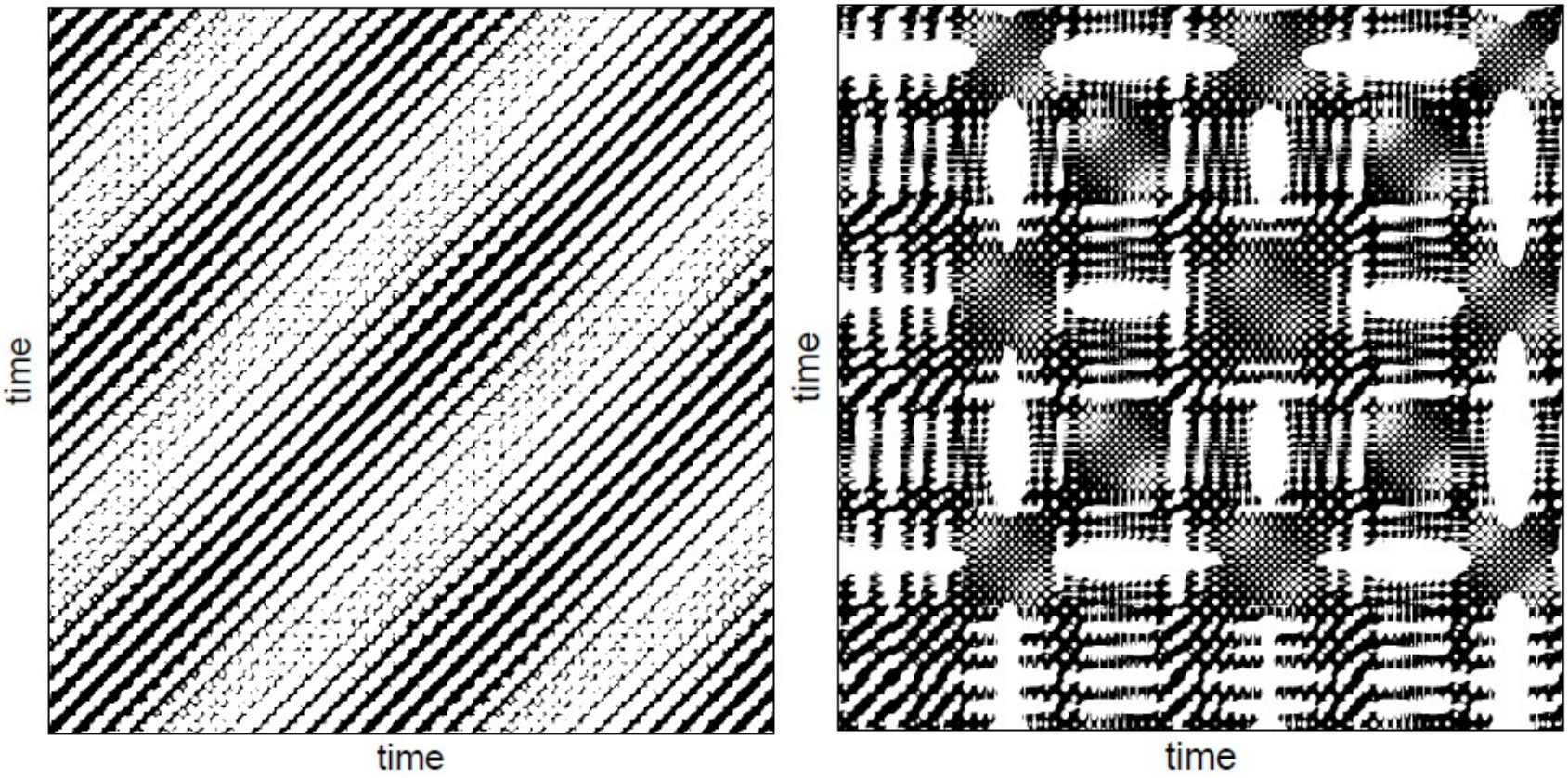

Figure: The recurrence plots (Kopacek et al. 2010) allow us to discriminate between regular vs. chaotic dynamics. Regular orbit $\rightarrow$ diagonal pattern (left). Chaotic orbit $\rightarrow$ complex structure (right).

Structures in RPs

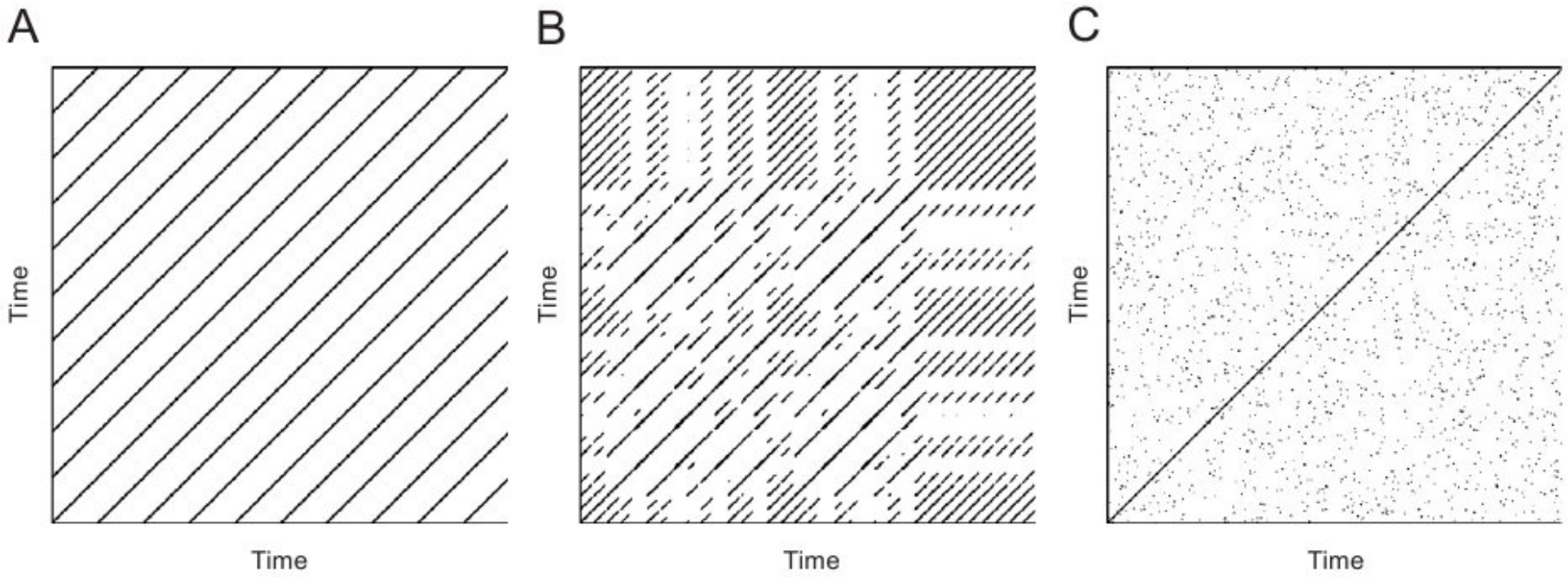

Figure: A – periodic motion with a single period, B – chaotic system, C – noise *(Marwan et al, 2006)*

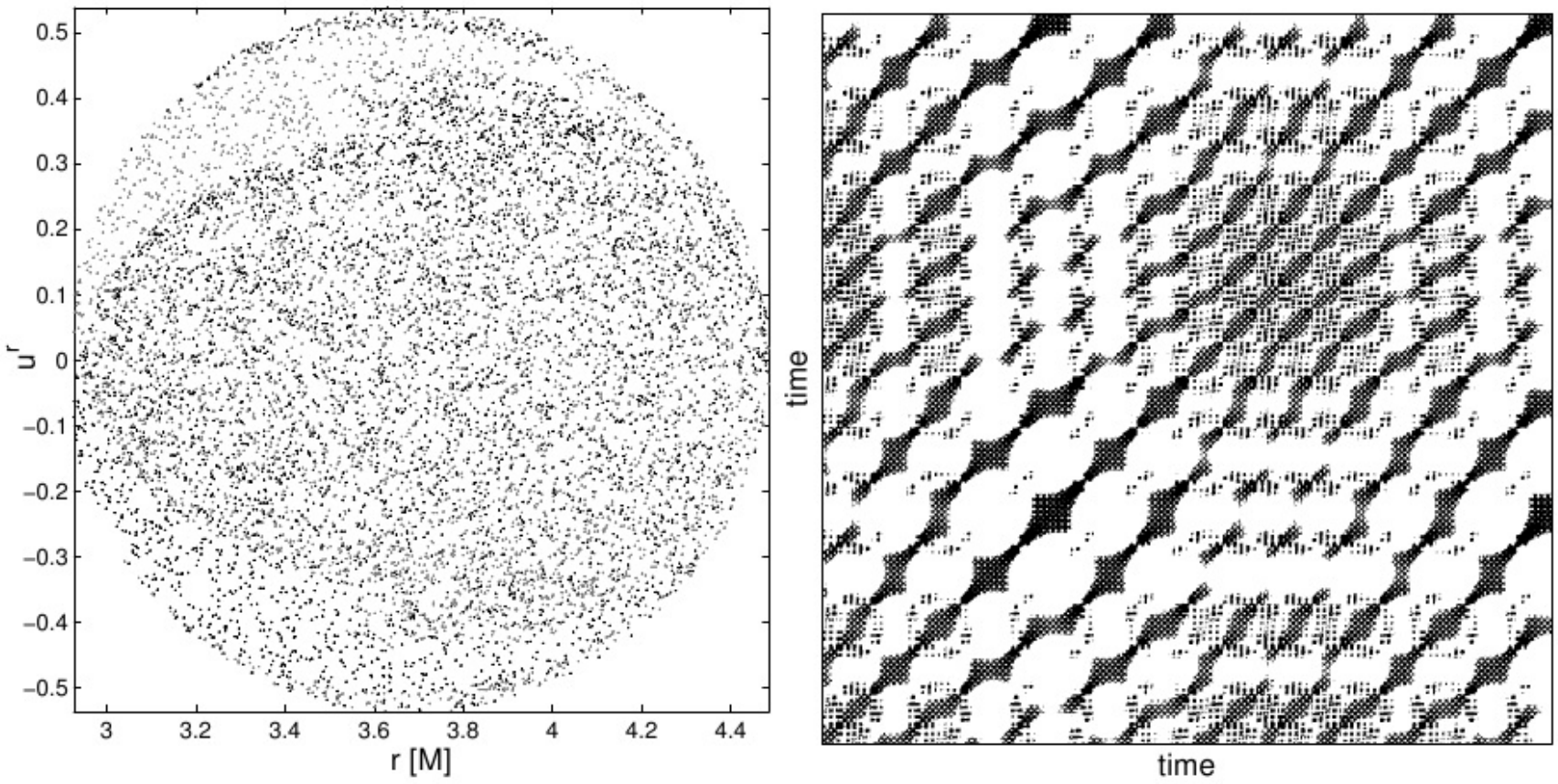

Figure: Poincaré sections for the case of particles, as their energy increases to $\tilde{E} = 1.75$.

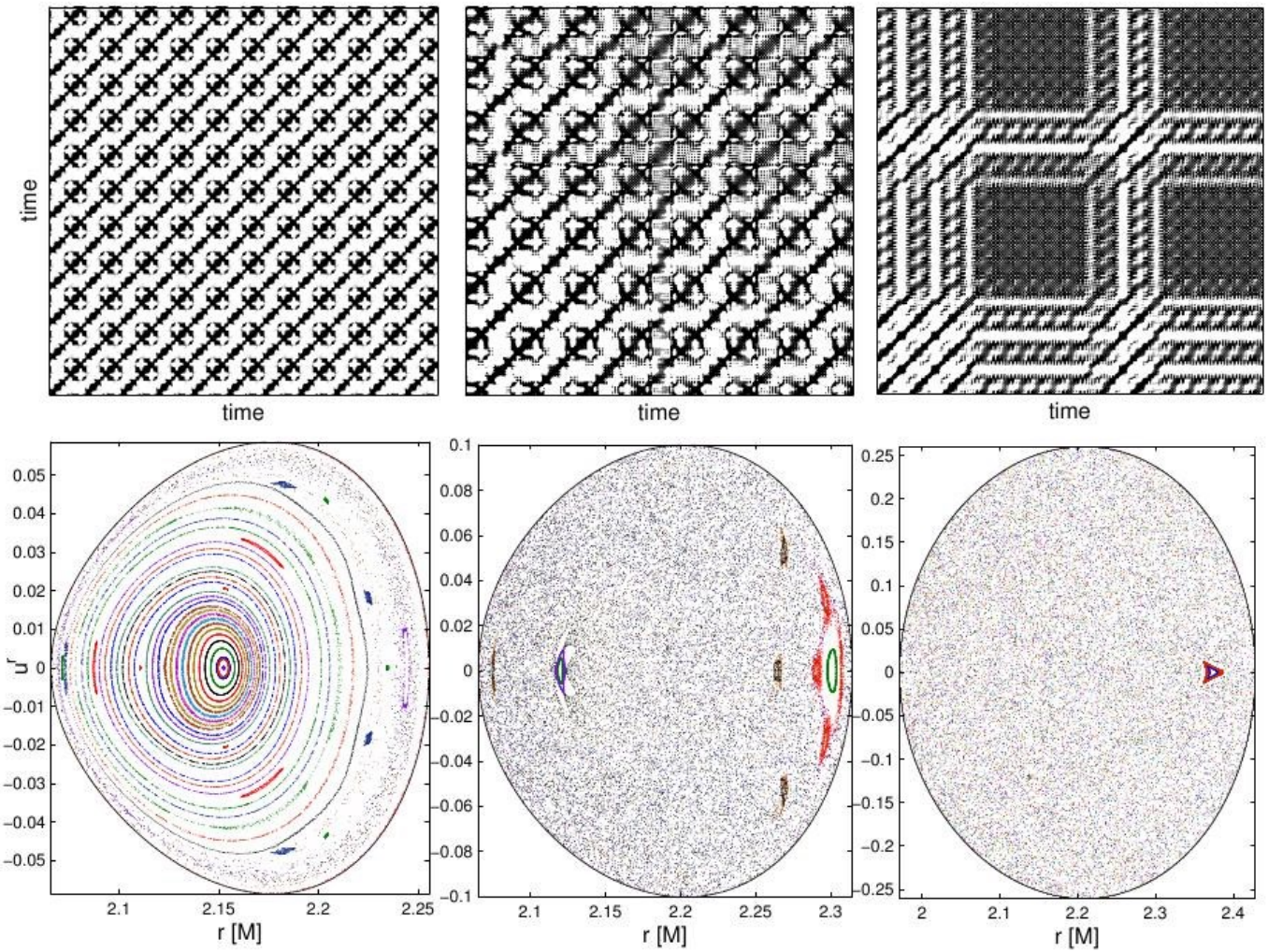

Figure: Comparison of trajectories of particles launched from the equatorial plane with different spin values. We have to link linearly the value of spin a with $\tilde{E}$ in order to maintain the existence of the potential lobe. In left panels we set $a = 0.5M$, $\tilde{E} = 1.795$, in middle panels $a = 0.6M$, $\tilde{E} = 1.92$ and in right panels $a = M$, $\tilde{E} = 2.42$.

Recurrence rate

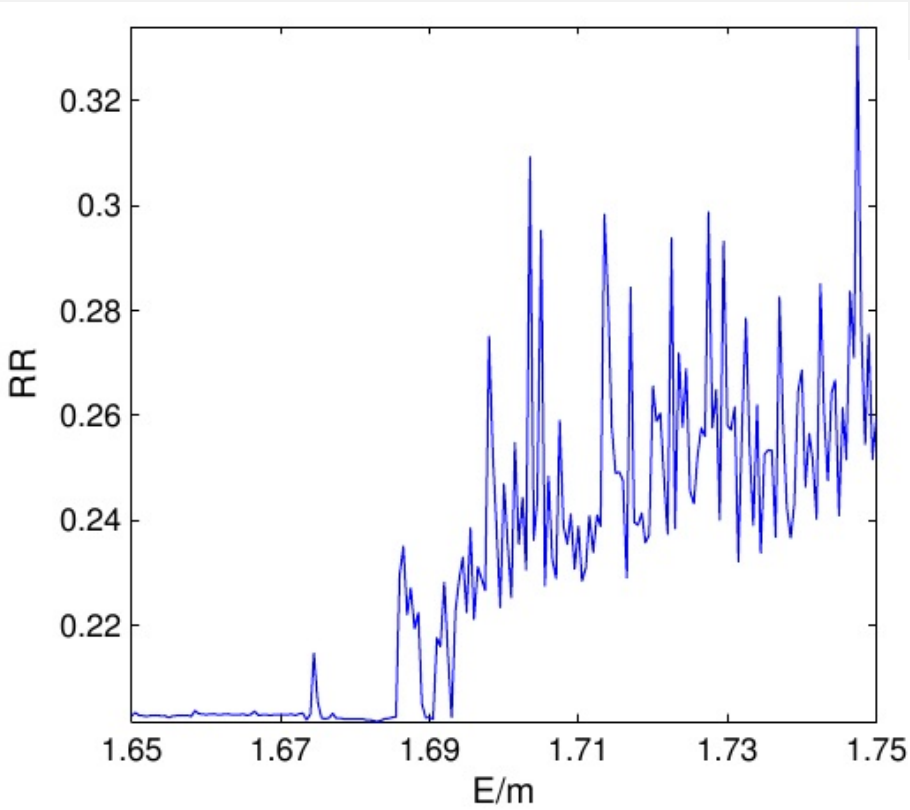

Recurrence rate (RR) as a function of specific energy $\tilde{E}$,

$$RR(\varepsilon) \equiv \frac{1}{N^2} \sum_{i,j=1}^{N} \mathbf{R}_{i,j}(\varepsilon)$$

Change of the pattern at $\tilde{E} \approx 1.685 \rightarrow$ this is where the chaos starts.

Thank you!

Further details: Kopáček O., & Karas V. (2018), "Near-horizon structure of escape zones of electrically charged particles around weakly magnetized rotating black hole", ApJ, 853, id. 53 (arXiv:1801.01576)

Discussion slides

Recurrence plot (RP)

$$\mathbf{R}_{ij} = \begin{cases} 1 & \text{black dot} \\ 0 & \text{white dot} \end{cases}$$

- RP is symmetric and the main diagonal is always occupied by the line of identity (LOI)
- vertical (horizontal) lines – slowly changing (laminar) states
- diagonal lines – paralelly evolving states – typical for integrable systems (broken diagonals are hallmark of chaos)

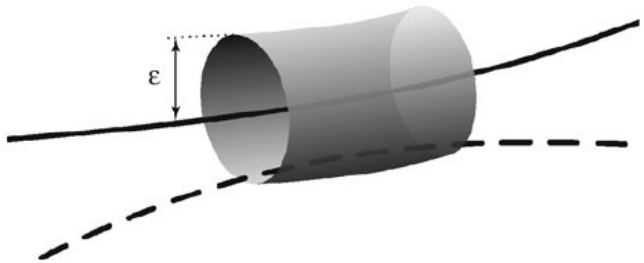

Properties of RPs

- simple construction regardless the dimension of the phase space (no section – all
- widely used for experimental data (including cardiology, economics etc) where just a fraction (or just one) of phase space coordinates is known from the measurement – Takens' embedding theorem allows to reconstruct the dynamics of the system
- structures in the RP encode surprisingly large amount of information – reconstruction of an attractor from RP is possible (Thiel et al, 2004)
- RPs allow to decide whether the motion is regular or chaotic – alternative tool to Poincaré surfaces of section when dealing with single trajectories

Recurrence quantification analysis (RQA)

- recurrence rate RR – density of points in RP

$$RR(\varepsilon) \equiv \frac{1}{N^2} \sum_{i,j=1}^{N} \mathbf{R}_{i,j}(\varepsilon)$$

- histogram $P(\varepsilon, l)$ recording the number of diagonal lines of length l

$$P(\varepsilon, l) = \sum_{i,j=1}^{N} (1 - \mathbf{R}_{i-1,j-1}(\varepsilon))(1 - \mathbf{R}_{i+l,j+l}(\varepsilon)) \prod_{k=0}^{l-1} \mathbf{R}_{i+k,j+k}(\varepsilon)$$

- $$DET \equiv \frac{\sum_{l=l_{\min}}^{N} lP(l)}{\sum_{l=1}^{N} lP(l)}, \quad L \equiv \frac{\sum_{l=l_{\min}}^{N} lP(l)}{\sum_{l=l_{\min}}^{N} P(l)}, \quad DIV \equiv \frac{1}{L_{\max}}$$

Notes to DIV

- intuition (supported by Eckmann, 1987): direct relation of *DIV* to the largest positive Lyapunov characteristic exponent $\lambda_{\max}$
- theoretical consideration: DIV is only an estimator for the lower limit of the sum of the positive Lyapunov exponents (Marwan, 2006)
- nevertheless *DIV* and $\lambda_{\max}$ appear to have good correlation in numerical simulation (Trulla et al, 1996)
- major drawback (cost we pay for its simplicity) of RPs and RQA: lack of invariance (dependence on the threshold ε, $l_{\min}$, choice of the norm etc.)

Trajectories in potential well

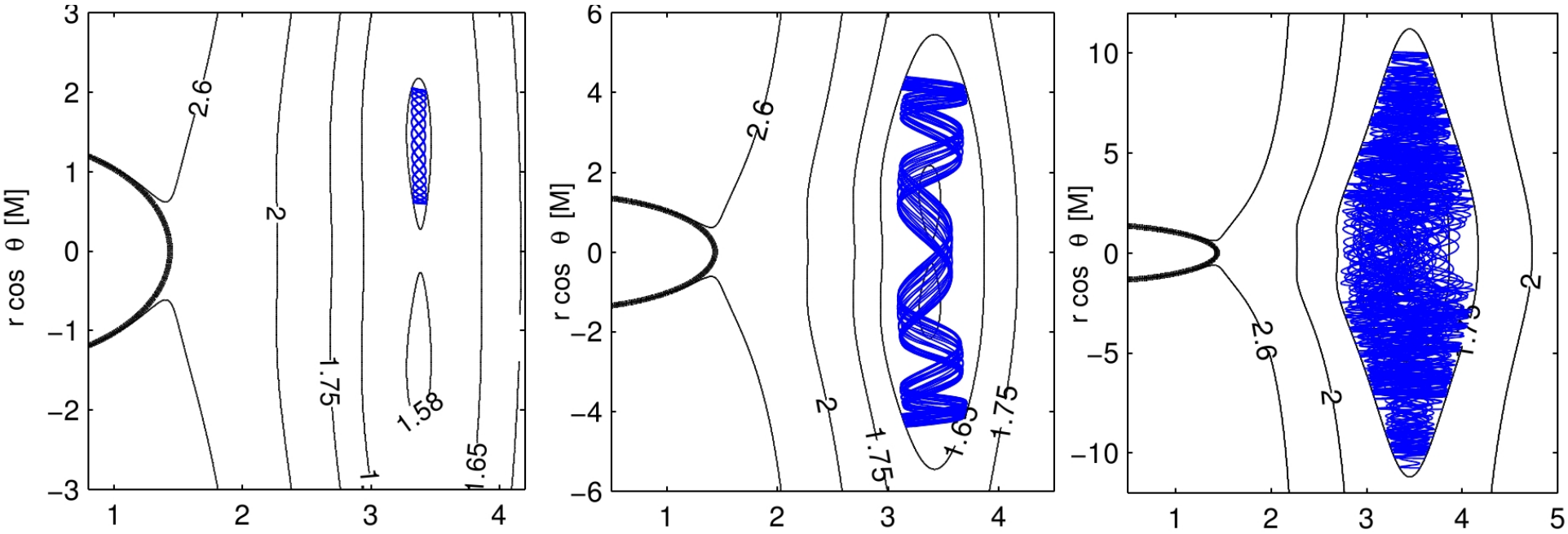

Figure: The test particle is launched from the locus of the off-equatorial potential minima with various values of the energy $\tilde{E}$. In the left panel we set $\tilde{E} = 1.58$ and we observe ordered off-equatorial motion. For the energy of $\tilde{E} = 1.65$ cross-equatorial regular motion is observed (middle panel). Finally in the right panel with $\tilde{E} = 1.75$ we observe irregular motion whose trajectory would ergodically fill whole allowed region after the sufficiently long integration time. We will show that the motion is chaotic in this case. Spin of the black hole is $a = 0.9\,M$ and its event horizon is depicted by the bold line.

Chaotic escape from the accretion disk – Poincaré section

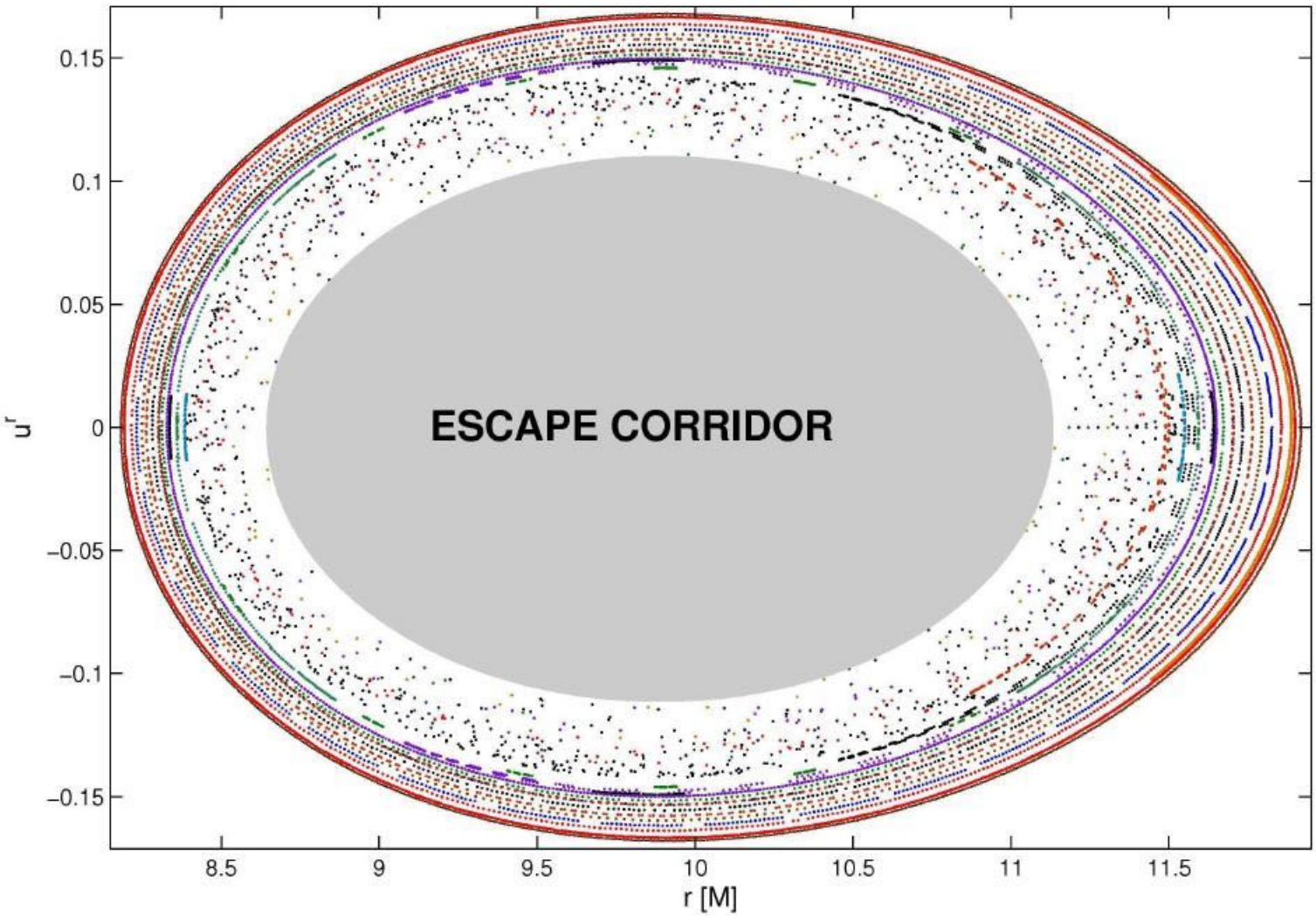

The Poincaré surface of section: $\theta_{\rm sec} = \pi/2$, $u^r(0)$.
Grey colour $\rightarrow$ the escape corridor from the equatorial plane.

- (Newtonian) **Kepler problem** is integrable → no chaos
- **Non-integrable perturbation**: by adding an axisymmetric or triaxial potential → domains of chaos emerge
- EXAMPLE: **Kirkwood gaps** in the main-belt asteroids – resonances with Jupiter → planet crossing orbits show chaos

these four initial values, the trajectory can be integrated to the next point satisfying (9), which is P_{i+1}.] It can also be shown that the mapping is area-preserving [see, e.g., Birkhoff (1927, p. 152); and see Moser (1962) for an important theorem concerning such mappings].

3. RESULTS

After some trials, the following potential was chosen for study:

$$U(x,y)=\tfrac{1}{2}(x^2+y^2+2x^2y-\tfrac{2}{3}y^3) \qquad (11)$$

because: (1) it is analytically simple; this makes the computation of the trajectory easy; (2) at the same time, it is sufficiently complicated to give trajectories which are far from trivial, as will be seen below. It seems probable that the potential (11) is a typical representative of the general case, and that nothing would be fundamentally changed by the addition of higher-order terms.

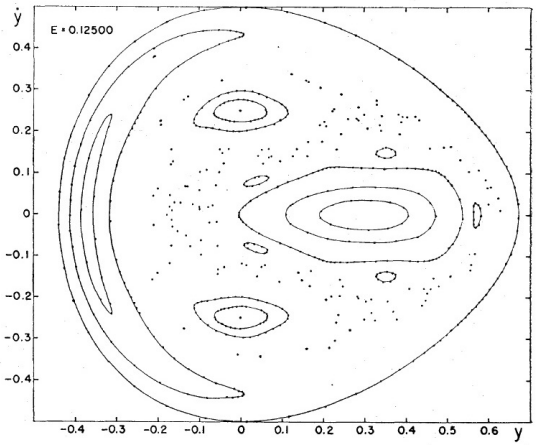

FIG. 5. Results for $E=0.12500$.

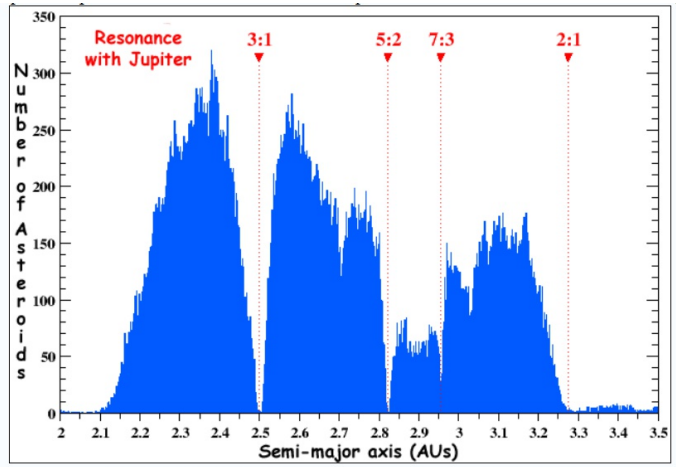

Kirkwood Gaps (after a diagram by Alan Chamberlain, CalTech, NASA/JPL)
(Plot of 157,000 asteroid semi-major axes, in 0.0005 AU increments)

Chaos in dynamical systems

- **Deterministic evolution**: equations of motion; no randomness
- **Chaos**: "*When the present determines the future, but the approximate present does not approximately determine the future*"
  Butterfly effect: *"Does the flap of a butterfly's wings in Brazil set off a tornado in Texas?"* (Lorentz 1972)
- **Exponential divergence** of neighbouring orbits:

$$|\delta Z(t)| \approx \mathrm{e}^{\chi t}|\delta Z(0)| \quad \ldots \quad \chi \text{ is the Lyapunov exponent}$$

- **Non-integrability**: "The applicability of the third integral of motion: Some numerical experiments" (Hénon & Heiles 1964)

$$V(x,y) = \frac{1}{2}\left(x^2+y^2\right) + k\left(x^2 y - \frac{y^3}{3}\right) \quad \ldots \rightarrow \text{chaotic dynamics}$$

detected in Poincaré sections

Chaotic motion near relativistic objects

- **Rotating (Kerr) black hole**: motion of particles *is integrable* $\rightarrow$ no chaos (Carter's constant of motion)
- **Magnetized (Ernst) black hole**: non-integrable perturbation $\rightarrow$ chaos onset (Karas & Vokrouhlický 1991; Li & Wu 2018)
- **Black holes with discs** (Semerák & Suková 2010)
- **The maximal Lyapunov exponent** $\rightarrow$ the most unstable direction (Lichtenberg & Lieberman 1992; Lukes-Gerakopoulos 2014)
- **Recurrence analysis** $\rightarrow$ alternative signature of chaos (Marwan et al. 2007)

Within GR framework the Lyapunov exponents are not invariant, however, they transform in such a way that positive Lyapunov exponents remain positive, and vice versa.

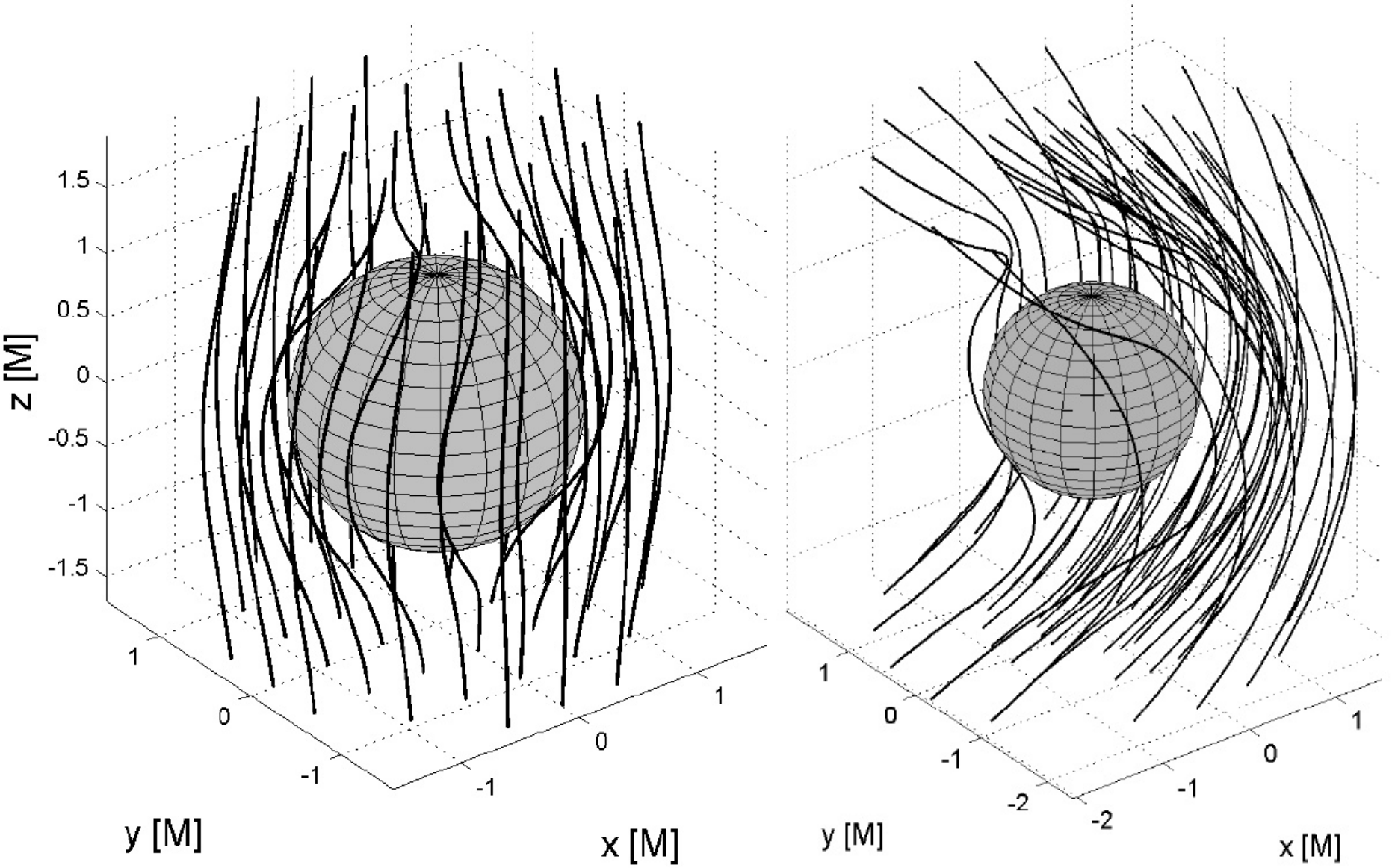

Figure: Two examples of organized magnetic fields near a rotating BH (Kopáček & Karas 2009, 2017).